ARCHIVIO ISTITUZIONALE DELLA RICERCA

Alma Mater Studiorum Università di Bologna
Archivio istituzionale della ricerca

Joint Sensing and Communications in Finite Block-Length Regime

This is the final peer-reviewed author's accepted manuscript (postprint) of the following publication:

*Published Version:*
Zabini, F., Paolini, E., Xu, W., Giorgetti, A. (2022). Joint Sensing and Communications in Finite Block-Length Regime [10.1109/GLOBECOM48099.2022.10001119].

*Availability:*
This version is available at: https://hdl.handle.net/11585/916473 since: 2024-02-23

*Published:*
DOI: http://doi.org/10.1109/GLOBECOM48099.2022.10001119

*Terms of use:*

Some rights reserved. The terms and conditions for the reuse of this version of the manuscript are specified in the publishing policy. For all terms of use and more information see the publisher's website.

This item was downloaded from IRIS Università di Bologna (https://cris.unibo.it/).
When citing, please refer to the published version.

(Article begins on next page)

21 January 2025

# Joint Sensing and Communications in Finite Block-Length Regime

Flavio Zabini†, Enrico Paolini†, Wen Xu‡, and Andrea Giorgetti†
† Wireless Communications Laboratory, CNIT, DEI, University of Bologna, Italy
‡Munich Research Center, Huawei Technologies Duesseldorf GmbH, Munich, Germany

***Abstract*—Systems that combine sensing and communication functionalities are gaining interest for several possible applications related to the internet of things (IoT) and the upcoming 6G mobile radio networks. Studies have recently been proposed to find the optimal tradeoff between sensing and communication performance. However, these studies assume continuous transmission and thus consider that the time available for estimation can always be large enough to achieve some desired accuracy. Moreover, in line with this assumption, communication performance is measured via the well-known Shannon capacity, which implicitly assumes indefinitely long error correction codes. However, in the case of short packet transmissions, such as the case in several IoT applications, the above assumption is unrealistic, as the length of the transmitted packet limits that of the error correction code and the observation time for parameter estimation. Therefore, this paper aims at investigating the optimal tradeoff between the data transmission and the target localization capabilities in a finite block-length regime, by making use of some typical metrics of the finite length information theory. In particular, the optimal beamforming, which minimizes the Cramér Rao bound of target localization, is derived under a constraint over the block error probability for given packet length values.**

## I. Introduction

Sensing capabilities via radio frequency signals have recently attracted an increasing interest for various applications, such as intelligent transportation, safety, assisted living, and human-machine interface [1]–[3]. Therefore, there is an increasing demand for systems exhibiting both sensing and communications functionalities, which will be a crucial goal for the next generation of mobile systems. Three different categories of architectures can be identified based on how radar and communications coexist:

- Coexistence in spectral overlap, when the communication and the radar systems use the same radio resources at the same time;
- Coexistence via cognition, when the communication and the radar transmitters use the same spectral resources at different times by applying cognitive radio principles;
- Functional coexistence, when only one active transmitter performs both radar and communication functionalities (no interference is produced and no real resource negotiation takes place).

We focus on the last category, which relies on combining radar and communication functionalities in the same hardware platform. In particular, the transmitted waveform is designed in a way that can convey information and, at the same time, has good properties for supporting sensing. In such a perspective multiple input - multiple output (MIMO) systems are of particular interest because, besides their well-known advantages on the communication side, more recently they have been proven to be effective also for sensing tasks [4]–[7]. For a MIMO system with joint communication and sensing (JCS) capabilities, the design of the transmitted beam pattern is crucial since a trade-off between detection/localization of the target and data transmission toward the communication users must be set. In general, the beam pattern which maximizes the sensing performance focalizes the transmitted power in the direction of the target. Differently, for what concerns communication performance, the beam should be designed to maximize the signal-to-noise ratio (SNR) or signal-to-interference plus noise ratio (SINR) of the user.

Several works have recently been dedicated to solve the so-called JCS trade-off [8]–[13]. However, few of these works have found analytical expressions. In particular, [14] considers a scenario where a MIMO base-station (BS) has to detect a single target while it is transmitting data to a certain number of users. For each instantiation of the channel coefficients, an analytical solution is proposed to express the trade-off between the detection probability and the achievable sum rate of the users. However, the resulting expression also involves quantities that must be calculated by adopting a golden search algorithm. In [15], a similar scenario is investigated, and the optimal trade-off between the localization and communication performance is analyzed. In particular, the MIMO dual function BS is considered to work as a mono-static radar, and the Cramér-Rao Bound (CRB) for the estimation of the target direction is adopted as the sensing performance indicator. Therefore, the optimal waveform is the one minimizing the CRB under the constraint over the SINR of the users. A closed-form analytical solution is found for the single-user case, for both point and extended targets. In contrast, for the multiuser case, a numerical algorithm is proposed.

The above-mentioned works calculate the JCS trade-off by implicitly assuming that, while the radar performance is limited by the length of the frame used for the localization/detection, the communication function can rely on the possibility of adopting indefinitely long codes. Indeed, the Shannon capacity, as well as the SINR (directly related to the capacity in the case of Gaussian regime), can provide

This work has been carried out in the framework of the CNIT National Laboratory WiLab and the WiLab-Huawei Joint Innovation Center.

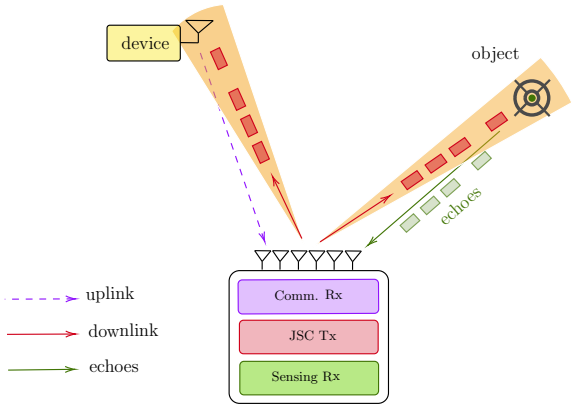


Fig. 1. Packet-based joint sensing and communication system.

meaningful information about the achievable data rate only in a classical information theory setting. In a typical internet of things (IoT) scenario, instead, where the communication is often based on short packet transmissions, the effects of a limited error correction code-length arise. In such a case, the so-called finite-length information theory provides more appropriate performance indicators [16], [17].

In this work, we consider a scenario similar to [14], [15] and focus our attention on the single-user case to obtain closed-form results for the trade-off between the localization performance and the block error probability for a fixed code length. Furthermore, we also consider an expression of the CRB that takes into account not only the estimate of the direction of the target but also that of the range; therefore more significant as it refers to the estimate of the position.

## II. System Model

Consider a dual function radar communication MIMO BS with antenna arrays of $N_\mathrm{t}$ and $N_\mathrm{r}$ elements at the transmitter and at the receiver side, respectively, with $N_\mathrm{t} < N_\mathrm{r}$. In such a system, the transmitted signal is used for both communication and radar purposes. For simplicity, we consider a scenario where a single target has to be tracked by the dual function waveform that carries information to a single user. A packet transmission is considered, with length $L$. The system model is exemplified in Fig 1.

### A. Radar Functionality

A mono-static configuration is considered so that the direction of departure of the radar signal coincides with the direction of arrival of the echo. We denote by $\theta$ the azimuth angle of the radar echo signal with respect to the BS and by $d$ the distance between the BS and the target. The sensing function is aimed at estimating the position $(x, y)$ of the target, where $x = d\sin\theta$ and $y = d\cos\theta$. However, according to [4], [5], the parameters that can be directly estimated by the BS are the angle of arrival (and departure) $\theta$ and the reflection coefficient $\alpha$, which captures both the roundtrip path-loss and the radar cross-section. By considering the radar equation in free space propagation we have

$$|\alpha|^2 = \sigma^2 d^{-4} \tag{1}$$

with $\sigma^2 \triangleq \frac{\rho\,\lambda^2}{(4\pi)^3}$ where $\rho$ is the radar cross-section (RCS) of the target and $\lambda$ is the wavelength. Denote as $\mathbf{X} \in \mathbb{C}^{N_\mathrm{t}\times L}$ the narrowband dual function radar-communication signal matrix, where $L$ is the frame length. We assume $L \geq N_\mathrm{t}$. For the radar purpose, the element $x_{i,j}$ of $\mathbf{X}$ is the $j$-th fast-time snapshot transmitted at the $i$-th antenna (see [14], [15]). We can write the reflected echo signal $N_\mathrm{r} \times L$ matrix as

$$\mathbf{Y}_\mathrm{R} = \alpha\mathbf{A}(\theta)\mathbf{X} + \mathbf{Z}_\mathrm{R} \tag{2}$$

where each element $y_{\mathrm{R}i,j}$ is the $j$-th fast-time snapshot received at the $i$-th antenna, $\mathbf{Z}_\mathrm{R}$ is the additive white Gaussian noise (AWGN) matrix, with covariance $\frac{1}{L}\mathbb{E}\left\{\mathbf{Z}_\mathrm{R}^H\mathbf{Z}_\mathrm{R}\right\} = \sigma_\mathrm{R}^2\mathbf{I}_{L\times L}$ ($\mathbf{I}_{L\times L}$ is the $L \times L$ identity matrix) and $\mathbf{A}(\theta) \in \mathbb{C}^{N_\mathrm{r}\times N_\mathrm{t}}$ is a matrix depending on the direction of arrival $\theta$ through the departure and arrival steering vectors $\mathbf{a}(\theta) \in \mathbb{C}^{N_\mathrm{t}\times 1}$ and $\mathbf{b}(\theta) \in \mathbb{C}^{N_\mathrm{r}\times 1}$ [5]. In particular

$$\mathbf{A}(\theta) \triangleq \mathbf{b}(\theta)\mathbf{a}^H(\theta) \tag{3}$$

where, for half-wavelength inter-element spacing

$$\mathbf{a}(\theta) \triangleq \left[e^{-j\frac{N_\mathrm{t}-1}{2}\pi\sin\theta}e^{-j\frac{N_\mathrm{t}-3}{2}\pi\sin\theta},\ldots,e^{j\frac{N_\mathrm{t}-1}{2}\pi\sin\theta}\right]^T \tag{4a}$$

$$\mathbf{b}(\theta) \triangleq \left[e^{-j\frac{N_\mathrm{r}-1}{2}\pi\sin\theta},e^{-j\frac{N_\mathrm{r}-3}{2}\pi\sin\theta},\ldots,e^{j\frac{N_\mathrm{r}-1}{2}\pi\sin\theta}\right]^T. \tag{4b}$$

Note that, according to [15], we have chosen the center of the antenna arrays as the reference point, so that the following symmetry property is verified: given $a_i$ and $b_i$ the $i$-th elements of $\mathbf{a}(\theta)$ and $\mathbf{b}(\theta)$, respectively, the derivatives with respect $\theta$

$$\dot{\mathbf{a}}(\theta) \triangleq \frac{d\mathbf{a}(\theta)}{d\theta} = \left[-ja_1\frac{N_\mathrm{t}-1}{2}\pi\cos\theta, -ja_2\frac{N_\mathrm{t}-3}{2}\pi\cos\theta, \ldots, ja_{N_\mathrm{t}}\frac{N_\mathrm{t}-1}{2}\pi\cos\theta\right]^T \tag{5a}$$

$$\dot{\mathbf{b}}(\theta) \triangleq \frac{d\mathbf{b}(\theta)}{d\theta} = \left[-jb_1\frac{N_\mathrm{r}-1}{2}\pi\cos\theta, -jb_2\frac{N_\mathrm{r}-3}{2}\pi\cos\theta, \ldots, jb_{N_\mathrm{r}}\frac{N_\mathrm{r}-1}{2}\pi\cos\theta\right]^T \tag{5b}$$

are such that

$$\dot{\mathbf{a}}^H(\theta)\mathbf{a}(\theta) = \dot{\mathbf{b}}^H(\theta)\mathbf{b}(\theta) = 0,\ \forall\theta\,. \tag{6}$$

### B. Communication Functionality

For the communication purpose, the $(i, j)$-th element of the narrowband dual function radar-communication signal matrix $\mathbf{X}$ in (2) is the discrete signal sample transmitted at the $i$-th antenna and the $j$-th time slot. The signal received by the user can be written in a vector form as

$$\mathbf{y}_\mathrm{C} = (y_{\mathrm{C}1}, y_{\mathrm{C}2}, \ldots, y_{\mathrm{C}L})^T = \mathbf{X}^H\mathbf{h} + \mathbf{z}_\mathrm{C} \tag{7}$$

where $\mathbf{h} \triangleq (h_1, h_2, \ldots, h_{N_\mathrm{t}})^T \in \mathbb{C}^{N_\mathrm{t}\times 1}$ is the vector of the channel coefficients and $\mathbf{z}_\mathrm{C} = (z_{\mathrm{C}1}, z_{\mathrm{C}2}, \ldots, z_{\mathrm{C}L})^T \in \mathbb{C}^{L\times 1}$ the white Gaussian noise vector such that $\mathbb{E}\left\{|z_{\mathrm{C}i}|^2\right\} = \sigma_\mathrm{C}^2$ for all $i$. The SNR for the communication user is thus given by

$$\gamma = \frac{\|\mathbf{X}^H\mathbf{h}\|^2}{L\,\sigma_\mathrm{C}^2}\,. \tag{8}$$

For each instantiation of the communication channel, the maximum achievable transmission rate is given by the well known Shannon capacity formula

$$c|_{\mathbf{h}}(\gamma) = \log_2(1+\gamma)\ [\text{bits/channel use}] \tag{9}$$

that holds since, given $\mathbf{h}$, the Gaussian noise is the only random quantity in (7). The value in (9) can be averaged over several realizations of the channel $\mathbf{h}$ as done in [14]. This implies that instantaneous rate adaptation is performed at the transmitter on the basis of the realization of the channel $\mathbf{h}$ (which is assumed to be known to both transmitter and receiver).

### C. Dual Function Waveform

The narrowband dual function radar/communication matrix $\mathbf{X}$ appears in both (2) and (7) that are related, respectively, to the radar and the communication functionality and is thus the parameter to be designed for the joint sensing and communication optimization. We consider

$$\mathbf{X} = \mathbf{w}\,\mathbf{s}_\mathrm{C}^H \tag{10}$$

where $\mathbf{w} \triangleq (w_1, w_2, \ldots, w_{N_\mathrm{t}})^T \in \mathbb{C}^{N_\mathrm{t}\times 1}$ is the dual function beam-forming vector to be optimized and $\mathbf{s}_\mathrm{C} = (s_1, s_2, \ldots, s_L) \in \mathbb{C}^L \times 1$ is the data stream. Without loss of generality, we can assume that $\frac{1}{L}\mathbf{s}_\mathrm{C}^H\mathbf{s}_\mathrm{C} = 1$ such that

$$\mathbf{R}_X \triangleq \frac{1}{L}\mathbf{X}\mathbf{X}^H = \frac{1}{L}\mathbf{w}\mathbf{s}_\mathrm{C}^H\mathbf{s}_\mathrm{C}\mathbf{w}^H = \mathbf{w}\mathbf{w}^H\,. \tag{11}$$

This way, the transmission power constraint reflects over $\mathbf{w}$ only and we have

$$\frac{1}{L}\sum_{i=1}^{N_\mathrm{t}}\sum_{j=1}^{L}|x_{ij}|^2 = \frac{1}{L}\mathrm{tr}(\mathbf{X}\mathbf{X}^H) = \mathrm{tr}(\mathbf{w}\mathbf{w}^H) = \|\mathbf{w}\|^2 \le P_\mathrm{T}\,. \tag{12}$$

Note that the SNR (8) can thus be written as

$$\gamma = \frac{\mathbf{h}^H\mathbf{X}\mathbf{X}^H\mathbf{h}}{L\,\sigma_\mathrm{C}^2} = \frac{\mathbf{h}^H\mathbf{w}\mathbf{w}^H\mathbf{h}}{\sigma_\mathrm{C}^2} = \frac{\|\mathbf{h}^H\mathbf{w}\|^2}{\sigma_\mathrm{C}^2}\,. \tag{13}$$

### D. Short Packet Communication

First, we assume that the channel coefficients do not change during the transmission of the whole data frame. Second, we consider a short packet communication employing a block error correction code where the code length $n$ is limited by the frame length $L$ (i.e., $n \le L$). In such a scenario, the capacity (9) is no more meaningful, and the maximum achievable rate $r$ for a reliable communication can be inferred by the Strassen formula [16]–[18]

$$P_\mathrm{e} = Q\left\{\left[c - r + O\left(\frac{\log_2 n}{n}\right)\right]\sqrt{\frac{n}{V}}\right\} \tag{14}$$

where $P_\mathrm{e}$ is the block error probability, $Q(\cdot)$ denotes the Gaussian Q-function, $c$ is the Shannon capacity in bits/channel use, and $V$ is the channel dispersion [19].

## III. Communication vs Sensing Trade-Off

### A. Cramér-Rao bound

As is well-known, the CRB provides a lower bound for the estimation error variance. More specifically, given the Fisher information matrix (FIM) $\boldsymbol{\mathcal{I}}(\theta,\alpha)$ whose elements are obtained by the second partial derivatives of the log-likelihood function with respect to $\theta$ and $\alpha$, the mean square errors (MSEs) in the estimation of $\theta$ and $\alpha$, $\mathrm{MSE}_\theta$ and $\mathrm{MSE}_\alpha$, may be lower bounded as

$$\mathrm{MSE}_\theta \ge \mathrm{CRB}(\theta) \triangleq [\boldsymbol{\mathcal{I}}^{-1}(\theta,\alpha)]_{1,1} \tag{15}$$

$$\mathrm{MSE}_\alpha \ge \mathrm{CRB}(\alpha) \triangleq [\boldsymbol{\mathcal{I}}^{-1}(\theta,\alpha)]_{2,2} \tag{16}$$

where $[\boldsymbol{\mathcal{I}}^{-1}(\theta,\alpha)]_{1,1}$ and $[\boldsymbol{\mathcal{I}}^{-1}(\theta,\alpha)]_{2,2}$ are the elements on the main diagonal of the inverse matrix $\boldsymbol{\mathcal{I}}^{-1}(\theta,\alpha)$. The CRB in (15) has been evaluated in [5] and applied to the JCS scenario in [15]. However, to quantify the localization error that is related to the target position estimate, not only the azimuth angle $\theta$ has to be evaluated but also the distance $d$ (namely the coefficient $\alpha$). In other words, in a meaningful CRB definition, both (15) and (16) should be taken into account. Noticing that the two expressions cannot be directly summed (since the former is expressed in rad$^2$, while the latter is not), we use the following definition, based on the Cartesian coordinates instead of the polar ones

$$\mathrm{MSE}_x + \mathrm{MSE}_y \ge \mathrm{CRB}(x,y) \triangleq \mathrm{tr}(\boldsymbol{\mathcal{I}}^{-1}(x,y)) \tag{17}$$

where $\mathrm{MSE}_x$ and $\mathrm{MSE}_y$ are the MSEs in the estimation of the two coordinates, and $\boldsymbol{\mathcal{I}}^{-1}(x,y)$ is the FIM obtained by deriving the log-likelihood function with respect to $x$ and $y$.

*Lemma 1:* When the coordinates $x$ and $y$ are estimated by observing the received signal (2), the CRB is given by

$$\mathrm{CRB}(x,y) = \frac{(x^2+y^2)^3}{\sigma^2}\,\frac{\sigma_\mathrm{R}^2}{2L}\left(\frac{1}{\|\dot{\mathbf{b}}\|^2|\mathbf{a}^H\mathbf{w}|^2} + \frac{1}{4N_\mathrm{r}\,|\mathbf{a}^H\mathbf{w}|^2} + \frac{1}{4\|\dot{\mathbf{b}}\|^2}\frac{|\dot{\mathbf{a}}^H\mathbf{w}|^2}{|\mathbf{a}^H\mathbf{w}|^4}\right) \tag{18}$$

where $\mathbf{a}$, $\dot{\mathbf{a}}$, and $\dot{\mathbf{b}}$ are obtained by considering $\cos\theta = y/\sqrt{x^2+y^2}$ and $\sin\theta = x/\sqrt{x^2+y^2}$ in (4a), (5a), and (5b).

*Proof:* By following the method proposed in [5], it can be shown that, when $\theta$ and $\alpha$ are estimated by observing (2), the FIM results in

$$\boldsymbol{\mathcal{I}}(\theta,\alpha) = \begin{bmatrix}\mathcal{I}_{\theta,\theta} & \mathcal{I}_{\theta,\alpha}\\ \mathcal{I}_{\alpha,\theta} & \mathcal{I}_{\alpha,\alpha}\end{bmatrix} \tag{19}$$

where, by defining $\dot{\mathbf{A}}(\theta) \triangleq \frac{d\mathbf{A}(\theta)}{d\theta}$, it is

$$\mathcal{I}_{\theta,\theta} = \frac{2L}{\sigma_{\mathrm{R}}^2}|\alpha|^2 \mathrm{tr}\left(\dot{\mathbf{A}}^H(\theta)\mathbf{R}_X\dot{\mathbf{A}}(\theta)\right) \tag{20a}$$

$$\mathcal{I}_{\alpha,\alpha} = \frac{2L}{\sigma_{\mathrm{R}}^2} \mathrm{tr}\left(\mathbf{A}^H(\theta)\mathbf{R}_X\mathbf{A}(\theta)\right) \tag{20b}$$

$$\mathcal{I}_{\theta,\alpha} = \frac{2L}{\sigma_{\mathrm{R}}^2}\alpha^* \mathrm{tr}\left(\mathbf{A}^H(\theta)\mathbf{R}_X\dot{\mathbf{A}}(\theta)\right) \tag{20c}$$

$$\mathcal{I}_{\alpha,\theta} = \frac{2L}{\sigma_{\mathrm{R}}^2}\alpha \mathrm{tr}\left(\mathbf{A}^T(\theta)\mathbf{R}_X^*\dot{\mathbf{A}}^*(\theta)\right) . \tag{20d}$$

It is known that

$$\boldsymbol{\mathcal{I}}(x,y) = \mathbf{J}^T\boldsymbol{\mathcal{I}}(\alpha,\theta)\mathbf{J} \tag{21}$$

where $\mathbf{J}$ is the Jacobian of the transformation

$$\theta = \arctan\left(\frac{x}{y}\right), \quad |\alpha| = \frac{\sigma}{x^2+y^2} .$$

Thus, using the circular permutation and indicating as $(\cdot)^{-T}$ the matrix operations of transposition and inversion (whose order can be exchanged when the matrix is invertible), we can compute CRB as follows

$$\begin{aligned}\mathrm{CRB}(x,y) &= \mathrm{tr}(\boldsymbol{\mathcal{I}}^{-1}(x,y)) = \mathrm{tr}(\mathbf{J}^{-1}\boldsymbol{\mathcal{I}}^{-1}(\alpha,\theta)\mathbf{J}^{-T}) \\ &= \mathrm{tr}(\mathbf{J}^{-T}\mathbf{J}^{-1}\boldsymbol{\mathcal{I}}^{-1}(\alpha,\theta))\end{aligned} \tag{22}$$

where $\mathbf{J}^{-1}$ coincides with the Jacobian of the inverse transformation

$$x = \sqrt{\frac{\sigma}{|\alpha|}}\sin\theta, \quad y = \sqrt{\frac{\sigma}{|\alpha|}}\cos\theta .$$

It is immediate that $\mathbf{J}^{-1} = \begin{bmatrix} \sqrt{\frac{\sigma}{|\alpha|}}\cos\theta & -\frac{1}{2}\sqrt{\frac{\sigma}{|\alpha|^3}}\sin\theta \\ -\sqrt{\frac{\sigma}{|\alpha|}}\sin\theta & -\frac{1}{2}\sqrt{\frac{\sigma}{|\alpha|^3}}\cos\theta \end{bmatrix}$. Thus, from $\mathbf{M} \triangleq \mathbf{J}^{-T}\mathbf{J}^{-1} = \begin{bmatrix} \frac{\sigma}{\alpha} & 0 \\ 0 & \frac{\sigma}{4\alpha^3} \end{bmatrix}$ and $\boldsymbol{\mathcal{I}}^{-1}(\alpha,\theta) = \begin{bmatrix} \mathcal{I}_{\alpha,\alpha} & \mathcal{I}_{\alpha,\theta} \\ \mathcal{I}_{\theta,\alpha} & \mathcal{I}_{\theta,\theta} \end{bmatrix}$, we can write

$$\mathbf{M}\,\boldsymbol{\mathcal{I}}^{-1}(\alpha,\theta) = \frac{1}{\mathcal{I}_{\theta,\theta}\mathcal{I}_{\alpha,\alpha} - \mathcal{I}_{\theta,\alpha}\mathcal{I}_{\alpha,\theta}} \begin{bmatrix} \frac{\sigma}{\alpha}\mathcal{I}_{\alpha,\alpha} & \frac{\sigma}{\alpha}\mathcal{I}_{\alpha,\theta} \\ \frac{\sigma}{4\alpha^3}\mathcal{I}_{\theta,\alpha} & \frac{\sigma}{4\alpha^3}\mathcal{I}_{\theta,\theta} \end{bmatrix} . \tag{23}$$

Now, by substituting (23) in (22), the CRB results in

$$\mathrm{CRB}(x,y) = \frac{\sigma}{|\alpha|}\frac{\mathcal{I}_{\alpha,\alpha} + \frac{\mathcal{I}_{\theta,\theta}}{4|\alpha|^2}}{(\mathcal{I}_{\theta,\theta}\mathcal{I}_{\alpha,\alpha} - \mathcal{I}_{\theta,\alpha}\mathcal{I}_{\alpha,\theta})} . \tag{24}$$

From (3), it follows $\dot{\mathbf{A}} = \dot{\mathbf{b}}\mathbf{a}^H + \mathbf{b}\dot{\mathbf{a}}^H$. Thus, by using (11), the orthogonality property (6), and the invariance of the trace with respect to the circular permutation, (20) becomes

$$\mathcal{I}_{\theta,\theta} = \frac{2L}{\sigma_{\mathrm{R}}^2}|\alpha|^2\left(\|\dot{\mathbf{b}}\|^2|\mathbf{a}^H\mathbf{w}|^2 + \|\mathbf{b}\|^2|\dot{\mathbf{a}}^H\mathbf{w}|^2\right) \tag{25a}$$

$$\mathcal{I}_{\alpha,\alpha} = \frac{2L}{\sigma_{\mathrm{R}}^2}\left(\|\mathbf{b}\|^2|\mathbf{a}^H\mathbf{w}|^2\right) \tag{25b}$$

$$\mathcal{I}_{\theta,\alpha} = \frac{2L}{\sigma_{\mathrm{R}}^2}\alpha^*\left(\|\mathbf{b}\|^2\mathbf{a}^H\mathbf{w}\mathbf{w}^H\dot{\mathbf{a}}\right) \tag{25c}$$

$$\mathcal{I}_{\alpha,\theta} = \mathcal{I}_{\theta,\alpha}^* . \tag{25d}$$

Thus, by using (25) in (24), we can write the CRB as

$$\begin{aligned}\mathrm{CRB}(x,y) =& \frac{\sigma}{|\alpha|^3}\frac{\sigma_{\mathrm{R}}^2}{2L}\Big[\left(\|\mathbf{b}\|^2|\mathbf{a}^H\mathbf{w}|^2\right) \\ &+\frac{1}{4}\left(\|\dot{\mathbf{b}}\|^2|\mathbf{a}^H\mathbf{w}|^2 + \|\mathbf{b}\|^2|\dot{\mathbf{a}}^H\mathbf{w}|^2\right)\Big] \\ &\times\Big[\left(\|\dot{\mathbf{b}}\|^2|\mathbf{a}^H\mathbf{w}|^2 + \|\mathbf{b}\|^2|\dot{\mathbf{a}}^H\mathbf{w}|^2\right) \\ &\times\left(\|\mathbf{b}\|^2|\mathbf{a}^H\mathbf{w}|^2\right) - |(\|\mathbf{b}\|^2|\mathbf{a}^H\mathbf{w}||\dot{\mathbf{a}}^H\mathbf{w}|)|^2\Big]^{-1} \\ =& \frac{\sigma}{|\alpha|^3}\frac{\sigma_{\mathrm{R}}^2}{2L}\frac{\left(\|\mathbf{b}\|^2|\mathbf{a}^H\mathbf{w}|^2\right)}{\|\dot{\mathbf{b}}\|^2\|\mathbf{b}\|^2|\mathbf{a}^H\mathbf{w}|^4} \\ &+\frac{\sigma}{|\alpha|^3}\frac{\sigma_{\mathrm{R}}^2}{2L}\frac{1}{4}\frac{\left(\|\dot{\mathbf{b}}\|^2|\mathbf{a}^H\mathbf{w}|^2 + \|\mathbf{b}\|^2|\dot{\mathbf{a}}^H\mathbf{w}|^2\right)}{\|\dot{\mathbf{b}}\|^2\|\mathbf{b}\|^2|\mathbf{a}^H\mathbf{w}|^4}\end{aligned} \tag{26}$$

that results in (18) by noticing that, from (4b), it is $\|\mathbf{b}\|^2 = N_{\mathrm{r}}$. □

### B. Block Error Probability

For each instantiation of the channel vector $\mathbf{h}$, the communication channel amounts to a complex AWGN channel and, for the blocklength values of interest, the block error probability can be approximated (see [17] for the details) by

$$P_{\mathrm{e}|\mathbf{h}}(\gamma) \approx Q\left([c|_{\mathbf{h}}(\gamma) - r]\sqrt{\frac{n}{V|_{\mathbf{h}}(\gamma)}}\right) \tag{27}$$

where $c|_{\mathbf{h}}(\gamma)$ is given by (9), while the dispersion is evaluated in [19] as

$$V|_{\mathbf{h}}(\gamma) = \gamma\,\frac{\gamma+2}{(\gamma+1)^2}\log_2 e . \tag{28}$$

Note that $V|_{\mathbf{h}}(\gamma)$ depends on $\mathbf{h}$ through the SNR $\gamma$ as expressed in (13).

### C. Joint Optimization

If the transmitted packet is long enough to make the finite block-length effect negligible (i.e., $n \to \infty$), the frame length $L$ affects the radar performance (18) only, and the Shannon formula (9) can be used to quantify the communication performance. In such a scenario, the following lemma extends the result obtained in [15] for the CRB (15) to the case in which the considered CRB is the one defined in (18).

*Lemma 2:* For each instantiation of the channel $\mathbf{h}$, the dual function waveform $\mathbf{w}_{\mathrm{opt}}$ which minimizes the CRB (18), under

the power constraint (12) and given that the communication channel capacity (9) is not lower that a certain value $C$, results in

$$\mathbf{w}_{\text{opt}} = \begin{cases} \sqrt{P_{\text{T}}}\frac{\mathbf{a}}{\|\mathbf{a}\|}, & \text{if } P_{\text{T}}|\mathbf{h}^T\mathbf{a}|^2 > \Gamma N_{\text{t}}\sigma_{\text{C}}^2 \\ x_1\mathbf{u} + x_2\mathbf{a}_{\text{u}} & \text{otherwise} \end{cases} \tag{29}$$

where $\Gamma \triangleq 2^C - 1$, $\mathbf{u} \triangleq \frac{\mathbf{h}}{\|\mathbf{h}\|}$, $\mathbf{a}_{\text{u}} \triangleq \frac{\mathbf{a}-(\mathbf{u}^H\mathbf{a})\mathbf{u}}{\|\mathbf{a}-(\mathbf{u}^H\mathbf{a})\mathbf{u}\|}$ and

$$x_1 = \sqrt{\frac{\sigma_{\text{C}}^2\Gamma}{\|\mathbf{h}\|^2}}\frac{\mathbf{u}^H\mathbf{a}}{|\mathbf{u}^H\mathbf{a}|}, \quad x_2 = \sqrt{P_{\text{T}} - \frac{\sigma_{\text{C}}^2\Gamma}{\|\mathbf{h}\|^2}}\frac{\mathbf{a}_{\text{u}}^H\mathbf{a}}{|\mathbf{a}_{\text{u}}^H\mathbf{a}|}. \tag{30}$$

*Proof:* By definition, we have that

$$\begin{aligned} &\mathbf{w}_{\text{opt}} \triangleq \arg\min_{\mathbf{w}} \text{CRB}(x,y) \\ &\text{s.t. } c|_{\mathbf{h}}(\gamma) \geq C\,, \quad \|\mathbf{w}\|^2 \leq P_{\text{T}}\,. \end{aligned} \tag{31}$$

First, by using (9), the condition over the capacity becomes $\gamma \geq \Gamma$, that, thanks to (13), becomes

$$|\mathbf{h}^H\mathbf{w}|^2 \geq \Gamma\sigma_{\text{C}}^2\,. \tag{32}$$

Second, we can note that increasing the transmitted power is beneficial for both communication and radar purposes due to the absence of interfering users. More specifically, increasing $\|\mathbf{w}\|^2$ (for given $\mathbf{w}/\|\mathbf{w}\|$) simultaneously leads to a decrease of (18) and an increase of (9). Thus, the optimal weight vector has to exploit the total power budget (i.e., equality holds in the constraint (12)). From $\|\mathbf{w}_{\text{opt}}\|^2 = P_{\text{T}}$, it follows that the optimization is done only through the direction of the unit vector $\mathbf{w}/\|\mathbf{w}\|$ in the $N_{\text{t}}$ dimensional space. From (18) and (32) it is clear that the only three directions which have effects over the optimization problem (31) are those of $\mathbf{a}$, $\dot{\mathbf{a}}$, and $\mathbf{h}$. Thus we can write $\mathbf{w}_{\text{opt}} \in \text{span}\{\mathbf{a}, \dot{\mathbf{a}}, \mathbf{h}\}$ (an eventual component belonging to the null space would only subtract power without contributing to the CRB and the SNR). Note also that, due to the orthogonal property (6), $\dot{\mathbf{a}} \perp \mathbf{a}$ ($\dot{\mathbf{a}}$ and $\mathbf{a}$ also belong to the same plane). Thus, it can be proved that (18) is decreasing as $|\mathbf{a}^H\mathbf{w}|$ increases (given $|\mathbf{h}^H\mathbf{w}|$ and $\mathbf{w}^H\mathbf{w}$, the direction of $\mathbf{w}$ which maximizes $|\mathbf{a}^H\mathbf{w}|$ is the same that minimizes $|\dot{\mathbf{a}}^H\mathbf{w}|$). Hence, by (9), it is immediate that the problem (31) is equivalent to

$$\begin{aligned} &\mathbf{w}_{\text{opt}} = \arg\max_{\mathbf{w}} |\mathbf{a}^H\mathbf{w}| \\ &\text{s.t. } |\mathbf{h}^H\mathbf{w}|^2 \geq \Gamma\sigma_{\text{C}}^2\,, \quad \|\mathbf{w}\|^2 \leq P_{\text{T}}\,. \end{aligned} \tag{33}$$

The optimal weight vector (33) has been evaluated in [15] to be (29). □

Suppose that the entire packet is used for both radar and communication purposes and that the code length equals the frame length, i.e., $n = L$. We immediately notice from (18) and (27) that such a length impacts both the radar and the communication performance. Thus a novel trade-off should be evaluated, taking the finite blocklength regime effect into account.

*Theorem 1:* The optimal JCS tradeoff between the CRB and the block error probability with code length $n = L$ can be expressed, for each realization of the communication channel vector $\mathbf{h}$, in the following parametric form

$$P_{\text{e}\max}(\Gamma) \triangleq Q\left\{[\log_2(1+\Gamma) - r]\sqrt{\frac{(\Gamma+1)^2\,L}{\Gamma(\Gamma+2)\log_2 e}}\right\} \tag{34}$$

$$\begin{aligned} \text{CRB}|_{\mathbf{h}}(\Gamma) \triangleq &\frac{(x^2+y^2)^3}{\sigma^2}\,\frac{\sigma_{\text{R}}^2}{2L}\left(\frac{1}{\|\dot{\mathbf{b}}\|^2|\mathbf{a}^H\mathbf{w}_{\text{opt}}|^2}\right. \\ &\left. + \frac{1}{4N_{\text{r}}\,|\mathbf{a}^H\mathbf{w}_{\text{opt}}|^2} + \frac{1}{4\|\dot{\mathbf{b}}\|^2}\frac{|\dot{\mathbf{a}}^H\mathbf{w}_{\text{opt}}|^2}{|\mathbf{a}^H\mathbf{w}_{\text{opt}}|^4}\right) \end{aligned} \tag{35}$$

where $\mathbf{w}_{\text{opt}}$ is a function of $\Gamma$ and $\mathbf{h}$ defined by (29).

*Proof:* It can be verified that the function $P_{\text{e}}|_{\mathbf{h}}(\cdot)$ obtained by substituting (28) in (27) is decreasing with $\gamma$. Thus the condition $c_{\mathbf{h}}(\gamma) \geq C$ becomes

$$\gamma \geq \Gamma \Leftrightarrow P_{\text{e}}|_{\mathbf{h}}(\gamma) \leq P_{\text{e}\max}(\Gamma)\,. \tag{36}$$

As a consequence, the optimal weights evaluated by (29) are those which minimize the CRB (18) with the constraints (12) and (36). □

## IV. Numerical Results

In this section, we present numerical results obtained by averaging the analytical expressions for the channel capacity, the block error probability, and the CRB (that are all depending on the channel vector $\mathbf{h}$) over $10^5$ instantiations of $\mathbf{h}$, via Monte Carlo simulations. The elements of $\mathbf{h}$ are generated as zero mean complex Gaussian random variable with variance $\mathbb{E}\{|h_i|^2\} = (4\pi d_{\text{c}}/\lambda)^{-2}$ for all $i$. The considered system has a carrier frequency $f_0 = 1\,\text{GHz}$, a transmitted power $P_{\text{T}} = 30\text{dBm}$, a signal bandwidth of $20\,\text{MHz}$, and a noise power spectral density of $-174\,\text{dBm/Hz}$. Without loss of generality, the target position is assumed at coordinates $(0, d)$ with range $d = 50\,\text{m}$, while the communication distance is $d_{\text{c}} = 800\,\text{m}$. The considered radar cross section is $\rho = 1\ \text{m}^2$, while the number of transmitting and receiving antennas are, respectively, $N_{\text{t}} = 16$ and $N_{\text{r}} = 20$.

In Fig. 2 the JCS trade-off with and without taking the finite blocklength effect into account is shown. To obtain meaningful values, for the sensing performance indicator (abscissa), we use the squared root of the CRB (18) normalized by the distance $d$ between the BS and the target. As the communication performance indicator (y-axis), we use the data rate in bit per second obtained by multiplying the channel capacity (9) by the signal bandwidth $B$. Besides, we also plot the data rate obtained through (27) by fixing a block error probability $\overline{P_{\text{e}}} = 10^{-4}$. In both cases, the values are averaged over several realization of the channel $\mathbf{h}$.

It can be noticed that, as expected, the accuracy in the target localization is bounded by the required data rate in an appreciable way, for any frame length. For example, with a frame length $L = 1024$, relaxing the data rate requirement from about 300 to 250Mbit/s allows a decrease of the normalized root CRB from 0.02 to 0.015 (i.e., 20%). This is in accordance with the recent results in the literature on JCS, e.g.,

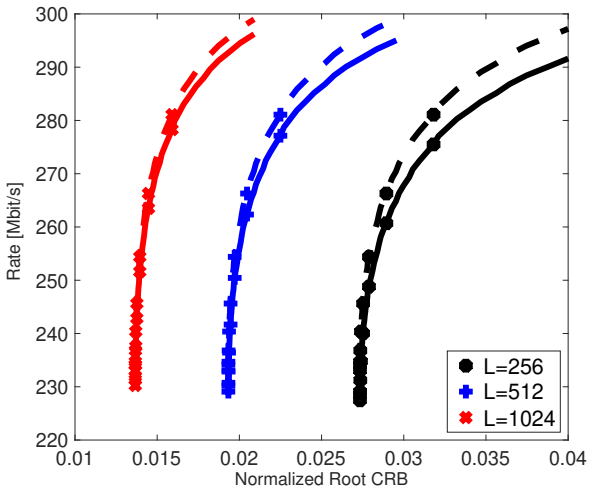


Fig. 2. Rate as a function of the normalized square root of the CRB varying the frame length $L$. Comparison between the capacity (dashed lines) and the maximum rate given $n = L$ and $P_{\text{emax}} = 10^{-4}$ (continuous lines).

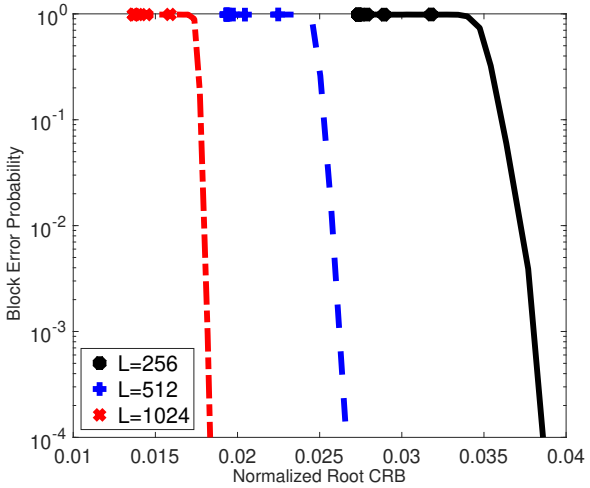


Fig. 3. Block error probability as a function of the normalized square root of the CRB varying the block length $n = L$, for a given bit rate of 290 Mbit/s.

those obtained in [14] and [15]. However, now we can also quantify the effect of the finite code length $n$ over the optimal JCS trade-off by observing the gap between the dashed lines (obtained for $n \to \infty$) and the continuous lines ($n = L$). For example, for $L = 512$ and a normalized root CRB of $0.025$, the achievable rate is about 5 Mbit/s less than the capacity. Such a gap increases for higher values of the CRB.

In Fig. 3 we plot the block error probability as a function of the normalized root CRB for different values of the code length (assumed equal to the frame length). The transmission rate is considered fixed to 290 Mbit/s. Here, rate adaptation is not performed, the zero-dispersion result provided in [20] holds and the error probability converges rapidly to the outage capacity It can be readily noticed that the finite blocklength regime effect dominates every other phenomenon. Indeed, the achievable localization accuracy is mainly determined by the value of $n = L$ and is not significantly affected by the requirement over the block error probability. For example, with all the considered values for the code (and frame) length $(256, 512, 1024)$, even accepting an increase of the block error probability by 3 or 4 orders of magnitude does not decrease the normalized root CRB of more than a small fraction (less than $0.01$). This is in accordance with the JCS literature that shows that, in general, the radar functionality is more critical than the communication one. Note that both Fig. 2 and Fig. 3 are obtained for a range of radar SNR $\gamma \in [20-45]$dB, that is, in the same working conditions of the JCS system considered in [15].

## V. Conclusion

In this paper, a packet-based joint sensing and communication system has been investigated. The optimal trade-off between radar and communication functionalities has been studied by means of finite-length information theory metrics, which is required in applications featuring finite packet lengths. We derived the analytical expression for the Cramér-Rao bound on the estimation of the target position and prove that the optimal waveform which minimizes the localization error can be evaluated as for the case without the code length restriction once such a parameter is taken into account in the block error probability constraint. Numerical results have shown that the effect of the finite code length dominates that of the constraint over the transmission quality.

## References


[1] A. Hassanien, M. G. Amin, Y. D. Zhang, and F. Ahmad, "Signaling strategies for dual-function radar communications: an overview," *IEEE Aerosp. Electron. Syst. Mag.*, vol. 31, no. 10, pp. 36–45, 2016.

[2] L. Zheng, M. Lops, Y. C. Eldar, and X. Wang, "Radar and communication coexistence: An overview: A review of recent methods," *IEEE Signal Process. Mag.*, vol. 36, no. 5, pp. 85–99, 2019.

[3] D. Ma, N. Shlezinger, T. Huang, Y. Liu, and Y. C. Eldar, "Joint radar-communication strategies for autonomous vehicles: Combining two key automotive technologies," *IEEE Signal Process. Mag.*, vol. 37, no. 4, pp. 85–97, 2020.

[4] E. Fishler, A. Haimovich, R. Blum, D. Chizhik, L. Cimini, and R. Valenzuela, "MIMO radar: an idea whose time has come," in *Proc. 2004 IEEE Radar Conf.*, 2004, pp. 71–78.

[5] I. Bekkerman and J. Tabrikian, "Target detection and localization using MIMO radars and sonars," *IEEE Trans. Signal Process.*, vol. 54, no. 10, pp. 3873–3883, 2006.

[6] P. Khomchuk, R. S. Blum, and I. Bilik, "Performance analysis of target parameters estimation using multiple widely separated antenna arrays," *IEEE Trans. Aerosp. Electron. Syst.*, vol. 52, no. 5, pp. 2413–2435, 2016.

[7] A. Sakhnini, M. Guenach, A. Bourdoux, and S. Pollin, "A Cramér-Rao lower bound for analyzing the localization performance of a multistatic joint radar-communication system," in *2021 1st IEEE Int. Online Symp. Joint Commun. Sensing*, 2021, pp. 1–5.

[8] C. Sturm and W. Wiesbeck, "Waveform design and signal processing aspects for fusion of wireless communications and radar sensing," *Proc. IEEE*, vol. 99, no. 7, pp. 1236–1259, 2011.

[9] P. Kumari, J. Choi, N. González-Prelcic, and R. W. Heath, "Ieee 802.11ad-based radar: An approach to joint vehicular communication-radar system," *IEEE Trans. Veh. Technol.*, vol. 67, no. 4, pp. 3012–3027, 2018.

[10] J. A. Zhang, X. Huang, Y. J. Guo, J. Yuan, and R. W. Heath, "Multibeam for joint communication and radar sensing using steerable analog antenna arrays," *IEEE Trans. Veh. Technol.*, vol. 68, no. 1, pp. 671–685, 2019.

[11] L. Pucci, E. Paolini, and A. Giorgetti, "System-level analysis of joint sensing and communication based on 5G new radio," *IEEE J. Sel. Areas Commun.*, 2022.

[12] F. Liu, C. Masouros, A. P. Petropulu, H. Griffiths, and L. Hanzo, "Joint radar and communication design: Applications, state-of-the-art, and the road ahead," *IEEE Trans. Commun.*, vol. 68, no. 6, pp. 3834–3862, 2020.

[13] P. Kumari, S. A. Vorobyov, and R. W. Heath, "Adaptive virtual waveform design for millimeter-wave joint communication–radar," *IEEE Trans. Signal Process.*, vol. 68, pp. 715–730, 2020.

[14] F. Liu, L. Zhou, C. Masouros, A. Li, W. Luo, and A. Petropulu, "Toward dual-functional radar-communication systems: Optimal waveform design," *IEEE Trans. Signal Process.*, vol. 66, no. 16, pp. 4264–4279, 2018.

[15] F. Liu, Y.-F. Liu, A. Li, C. Masouros, and Y. C. Eldar, "Cramer-Rao bound optimization for joint radar-communication beamforming," *IEEE Trans. Signal Process.*, vol. 70, pp. 240–253, 2022.

[16] M. Hayashi, "Information spectrum approach to second-order coding rate in channel coding," *IEEE Trans. Inf. Theory*, vol. 55, no. 11, pp. 4947–4966, 2009.

[17] Y. Polyanskiy, H. V. Poor, and S. Verdu, "Channel coding rate in the finite blocklength regime," *IEEE Trans. Inf. Theory*, vol. 56, no. 5, pp. 2307–2359, 2010.

[18] V. Strassen, "Asymptotische abschatzungen in Shannon's informations theorie," in *Trans. Third Prague Conf. Information Theory, Prague, Czech Republic,*, Jun. 1962, p. 689–723.

[19] Y. Polyanskiy, H. V. Poor, and S. Verdu, "Dispersion of Gaussian channels," in *Proc. 2009 IEEE Int. Symp. Inf. Theory*, 2009, pp. 2204–2208.

[20] W. Yang, G. Durisi, T. Koch, and Y. Polyanskiy, "Quasi-static multiple-antenna fading channels at finite blocklength," *IEEE Transactions on Information Theory*, vol. 60, no. 7, pp. 4232–4265, 2014.